

# Expanding Force in Astronomy and Updraft Force in Meteorology

WeiHong Qian

School of Physics, Peking University, Beijing, China

Email: [qianwh@pku.edu.cn](mailto:qianwh@pku.edu.cn)

**How to cite this paper:** Qian, W.H. (2025)

Expanding Force in Astronomy and Updraft Force in Meteorology. *Journal of Modern Physics*, **16**, 267-285.

<https://doi.org/10.4236/jmp.2025.162013>

**Received:** November 12, 2024

**Accepted:** February 10, 2025

**Published:** February 17, 2025

Copyright © 2025 by author(s) and

Scientific Research Publishing Inc.

This work is licensed under the Creative

Commons Attribution International

License (CC BY 4.0).

<http://creativecommons.org/licenses/by/4.0/>



Open Access

## Abstract

Astronomical extreme events or phenomena include black holes as well as nebulae systems that resemble the Milky Way. Meteorological extreme events or phenomena include tornadoes and tropical cyclones. The new high energy state of matter expanding outwards by spin jets from the two poles of an astronomical black hole, the new high energy state of matter in a funnel-shaped vortex showed a meteorological tornado expanding downwards from a rotated disk of cumulonimbus clouds, the new high energy state of matter in a tropical cyclone and the new high energy state of a nebulae system converging celestial materials are phenomena across disciplines and multiple time-space scales that have not yet been physically explained. In this paper, the theory of orthogonal collision in the rotational contraction continuum is used to unify the understanding of diverse extreme events or phenomena through a single dynamical mechanism, offering insights into natural processes across disciplines. In the field of astronomy, the orthogonal collision of two-beam rotating and contracting particles or stars associated with centripetal forces forms a new high-energy state of matter at the collision point and the new high-energy particles have expanding forces outward to both sides of the collision plane. In the field of meteorology, the orthogonal collision of multiple horizontally rotating and contracting airflows associated with centripetal forces forms a new high energy state of matter at the collision point as well as an updraft force and a downdraft force vertically. The updraft force and downdraft force formed by the collision of anomalous wet airflows in the lower atmosphere can well indicate tornado, thunderstorm and extreme precipitation. The orthogonal collision theory can be applied to explain new states of matter in disciplines from the astronomical scale to the meteorological scale and the Planck scale.

## Keywords

Astronomy, Meteorology, Black Hole, Tornado, Expanding Force, Updraft Force

## 1. Introduction

Collisions between objects can lead to destructive events. Two cars can form multi-angle collision events, such as rear-end collision, head-on collision, and right-angle collision events. The intensity of a collision event is closely associated with the mass, speed and angle of two cars moved. When two cars collide with acceleration, the energy density and breakage will be greater. There are two types of forces for a particle acceleration. One is the force of acceleration of the particle as a time function of speed. Another is the centripetal force of the change in the moving direction of the particle.

Since the Big Bang, the movement of matter or particles in nature has been characterized by two fundamental characteristics of accelerating expansion and bending motion [1]. If all matter or particles had accelerating straight-line expansion from the singularity of the Big Bang, it would have been impossible for them to collide. The collision is possible for matter or particles that expand at their accelerating rates with time and bending motions at the same time to converge at multiple angles in space. Earth fluids, including magmatic fluids, oceanic fluids, and atmospheric fluids, also exhibit the characteristics of bending motion, especially local vortex motion in these fluids. The density of the Earth's fluids decreases with the increase of distance from the Earth's center, so the Earth's fluids have the characteristics of vertical different layers and the large-scale horizontal motion on the spherical surface. The horizontal velocity of the Earth's fluids can be easy to measure. However, the horizontal velocity of the Earth's fluids is abnormal at sometimes, causing local formations in the abnormal energy density and vertical convective movements. The high anomalous energy and vertical convective motions inside Earth's fluids are difficult to be measured and calculated. The change in the vertical movement of the Earth's fluids is the direct cause of the occurrence of seismic volcano events, oceanic tide events, and atmospheric storm events [2] [3].

In astronomy, black holes and Milky Way-like celestial systems are also events with anomalous energy concentrated [4] [5]. A particularly difficult question to answer is why there are upward spin jets and downward spin jets of new material which are perpendicular to the black hole and the accretion disk. The same question is why there is a downward vortex namely tornado with huge energy density which is also perpendicular to the cumulonimbus cloud disk and the surface [6]-[8]. Another type of atmospheric extreme events comes from tropical cyclones such as super typhoons and super hurricanes [9]-[11].

Black holes and the Milky Way are astronomical scale events, while tornadoes and tropical cyclones are meteorological scale events. On time scales, the latter can be understood and analyzed through human observation from minutes to days. An ancient Greek philosopher Epicurus (340 - 271 bce) tried to explain a set of phenomena that are not directly reachable by empirical study because they happen at a remote distance from humans on Earth [12]. These include cosmological phenomena such as the shape and size of the universe, astronomical phenomena such as the rising and setting of the Sun, as well as meteorological and geological

phenomena such as thunder, lightning, and earthquakes. During that period, Epicureans did not typically offer single authoritative explanations for these individual phenomena, but instead have recourse to the idiosyncratic Epicurean doctrine of multiple explanation, where inaccessible phenomena are often given multiple possible explanations. This paper focuses on astronomical scale black hole extreme events and meteorological scale tornado extreme events, as well as Milky Way-like celestial systems and tropical storms, offering single theory to explain these individual phenomena.

## 2. The Expanding Force in a Black Hole and the Updraft Force in a Tornado

Black holes are the most extreme events in astronomy [13] [14]. Tornadoes are the most extreme events in meteorology [8] [15]. Black holes are recognized the direct consequences of gravity or follow the gravitational law and are explained by the general relativity, but there is still a lack of understanding and explaining the spatial structure and properties of events, especially the high-energy plasma spin jets expanded at the poles of black holes [16] [17]. The United States is one of the most tornado-prone regions on Earth, where a severe process of tornado outbreaks can kill hundreds of people [8] [18] [19]. In China, tornado occurs in isolation and can cause dozens of deaths and significant property damage [20].

For an astronomical black hole, the two extreme phenomena include the high energy density at its center and the high energy spin jets that expand outwards in the two poles [21]. For a meteorological single tornado, an extreme phenomenon is the funnel-shaped vortex expanding downwards from the rotating cumulonimbus cloud disk [22] [23]. These phenomena are scientific problems that have not been explained for a long time. **Figure 1(a)** shows an accretion disk of nebula material and a black hole with the vertical expanding polar plasma high energy spin jets. On the accretion disk, nebulous matter converges in a spiral plane towards the central point H. The closer to the black hole (the black dot in **Figure 1(a)**), the greater the mass-energy density there, and therefore the brighter it is. The two red dotted-line arrows indicate the contraction and convergence of nebula matter along their curved streamlines towards the black hole. Nebula matter moving along a curved streamline is subjected to a centripetal force, represented by a black arrow, pointing to the black hole point H. As the two curved streamlines contract to point H, the centripetal forces of particles A and B collide perpendicularly towards at point H.

Whether it is a celestial body that accelerates a rotational expansion or a celestial body that accelerates a rotational contraction, the force of particle motion has two components,

$$\mathbf{F} = \mathbf{F}_a + \mathbf{F}_p = m \, dv/dt \, \mathbf{k} + m(v^2/r) \mathbf{n} \quad (1)$$

where,  $\mathbf{F}_a = m \, dv/dt \, \mathbf{k}$  is the force with its vector  $\mathbf{k}$  that can cause the straight-line acceleration of a particle with its mass  $m$  and speed  $v$ , and  $\mathbf{F}_p = m(v^2/r) \mathbf{n}$  is

the centripetal force with its vector  $\mathbf{n}$  associated with the bending motion of the particle. The new particles formed after the Big Bang have the above two component forces. The forces of the particle straight-line acceleration cause the expansion of the universe, while the centripetal forces of the bending motion of the particles converge them into celestial bodies such as stars, planets, and moons, and even continue to converge them into new celestial systems such as the Milky Way [1]. Thus, each celestial body has different horizontal layers with increasing densities vertically to its center.

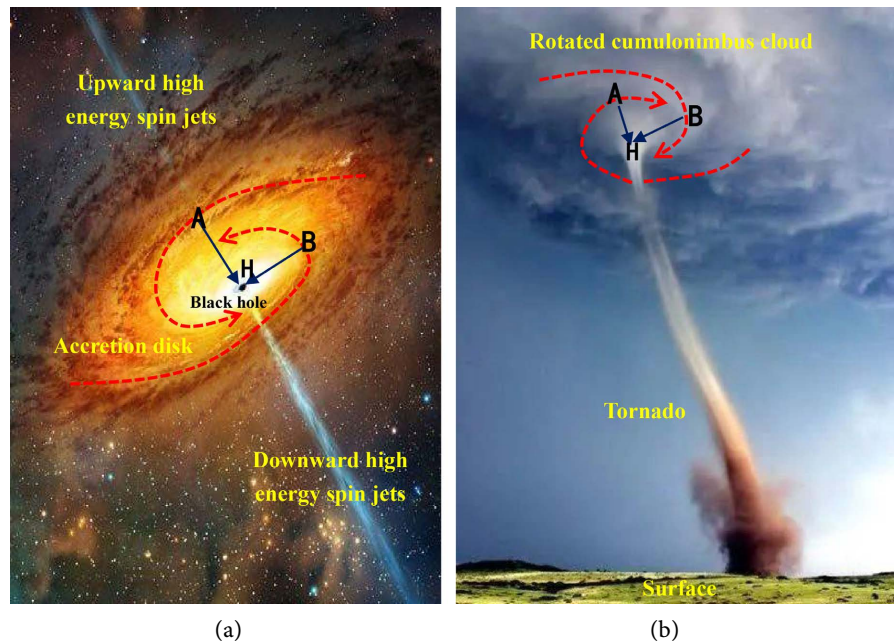


**Figure 1.** (a) An accretion disk of nebula materials and a black hole with its vertical expanding polar plasma spin jets. (b) A rotated disk of cumulonimbus clouds and a tornado (funnel-shaped vortex) expanding downward to the surface. The letter H indicates the area of high energy density surrounded by rotating and converging nebula materials in (a) and cumulonimbus clouds in (b). The two black arrows from two particles A and B are two centripetal forces associated with the curvilinear motion of nebula flows (red dashed arrows) in (a) and airflows (red dashed arrows) in (b).

The two particles A and B moving along the two curved streamlines have their centripetal forces,

$$\mathbf{F}_A = \frac{m_A}{r_A} v_A^2 \mathbf{n}_A, \quad (2)$$

and

$$\mathbf{F}_B = \frac{m_B}{r_B} v_B^2 \mathbf{n}_B. \quad (3)$$

where,  $m$  is a particle mass,  $v$  is its speed, and  $r$  is its moving radius at a direction  $\mathbf{n}$ . The new force  $\boldsymbol{\tau}_H$  generated by the cross collision of two particles along their streamlines to the point H is [1] [24],

$$\boldsymbol{\tau}_H = \left( \frac{m_A}{r_A} v_A^2 \right) \cdot \left( \frac{m_B}{r_B} v_B^2 \right) \cdot (\mathbf{n}_A \times \mathbf{n}_B). \quad (4)$$

Mathematically, the cross product of two forces (or vectors) should be a new force (or a new vector  $\boldsymbol{\tau}_H = \mathbf{F}_A \times \mathbf{F}_B$ ). The new force has two directions perpendicular to the collision plane of two moving particles along their streamlines. The term  $\frac{m_A}{r_A} v_A^2$  or  $\frac{m_B}{r_B} v_B^2$  is the mass-energy density per a unit length. The new force modulus produced by the collision is,

$$\tau_H = \left( \frac{m_A}{r_A} v_A^2 \right) \cdot \left( \frac{m_B}{r_B} v_B^2 \right) \sin \theta. \quad (5)$$

If the two centripetal forces are orthogonally interacted ( $\theta = 90^\circ$  degrees) with the same mass  $m$ , velocity  $v$  and radius  $r$ , the new force modulus reaches the maximum,

$$\tau_{Hmax} = (4/r^2) E_A E_B. \quad (6)$$

where,  $E = 1/2 mv^2$ . The product of mass-energy density for the orthogonal collision along their streamlines at the point  $H$  is  $4E^2$  per a unit area  $r^2$ . If  $\theta = 0^\circ$  or  $\theta = 180^\circ$  degrees, the product of mass-energy density is zero. If  $\theta = 90^\circ$  degrees, Equation (5) describes the product of mass-energy density for an orthogonal collider [25].

Just as the large number of particles in **Figure 1(a)** converge in spiral lines along each path of the red dashed-line arrows towards the center point  $H$  on the accretion disk, the black hole formed has a huge mass-energy density. If two old particles are taken with the same mass  $\tilde{m} = m_A = m_B$ , the same speed  $\tilde{v} = v_A = v_B$ , and the same radius  $\tilde{r} = r_A = r_B$ , then the mass-energy is also the same, *i.e.*,

$$\tilde{E} = \tilde{E}_A = \tilde{E}_B = 1/2 \cdot \tilde{m} \tilde{v}^2. \quad (7)$$

If taking  $\tilde{r} = 1$  as the unit length of the new state of matter, the product of mass-energy density per unit area  $\tilde{r}^2$  is,

$$\tau_{HM} = 4\tilde{E}^2. \quad (8)$$

The new state of matter with the high mass-energy density concentrates on a singularity of orthogonal collision. The mathematical singularity describes a physical new black hole. New materials and energy properties in the new universe after the orthogonal collision are unrelated to the materials and energy properties of the old universe before the orthogonal collision. The new particles no longer move around the old universal centrosome. In Equation (8), the term  $4\tilde{E}^2$  on the right-hand side is the new mass-energy density formed after the orthogonal collision of two old celestial bodies or two old particles, while the term  $\tau_{HM}$  on the left-hand side is the mass-energy density of all new particles in the new physical state. The two space-times or universes before and after the orthogonal collision are completely different.

In Equation (8), if there are  $N$  new particles in the new physical state of matter,

each particle has a mass  $m$  and a speed  $c$ . The total mass-energy of  $N$  new particles in the new universe is equivalent to the mass-energy of two old particles in the old universe,

$$4\tilde{E}^2 \Rightarrow Nmc^2. \quad (9)$$

where, the symbol “ $\Rightarrow$ ” indicates that the mass-energy of objects in the old universe is unidirectionally converted into the total mass-energy of  $N$  new particles in the new universe after the orthogonal collision. Apparently, there is an equivalence relationship,

$$E = mc^2 \quad (10)$$

where,  $E = 4\tilde{E}^2/N$  expresses the mass-energy of each new particle among total  $N$  new particles. Equation (10) expresses the mass-energy  $E$  of each new particle associated with its mass  $m$  and speed  $c$  in the new universe. The mass-energy  $E$ , mass  $m$  and speed  $c$  in the new universe are different from the mass-energy  $\tilde{E}$ , mass  $\tilde{m}$  and speed  $\tilde{v}$  in the old universe. The form of Equation (10) is the same as the mass-energy formula of Einstein [26]. However, the physical meaning of Equation (10) is different from the relationship of mass-energy equivalence which was based on the special theory of relativity or relativistic mathematical transformations of two coordinate systems [27]. Thereafter, the term  $mc^2$  or  $mv^2$  or  $\tilde{m}\tilde{v}^2$  is referred as mass-energy in different universes.

Between the new and old universes, the conversion relationship of mass-energy is physically like,

$$\tilde{m}_A \tilde{v}_A^2 \cdot \tilde{m}_B \tilde{v}_B^2 \Rightarrow Nmc^2. \quad (11)$$

Equation (11) describes the conversion of mass-energy from an old universe (left) to a new universe (right) through the orthogonal collision. Equation (9) or Equation (11) shows that there is only a one-way conversion from the mass ( $\tilde{m}_A, \tilde{m}_B$ ) with their velocities ( $\tilde{v}_A, \tilde{v}_B$ ) in the old universe to the total energy ( $Nmc^2$ ) in the new universe, but there is no information exchange between them. In Equation (11),  $m \ll \tilde{m}_A$  ( $\tilde{m}_B$ ) and  $c \gg \tilde{v}_A$  ( $\tilde{v}_B$ ).

In Equation (11), the orthogonal collision of two old particles forms  $N$  new particles. In **Figure 1(a)**, half of the new particles,  $N/2$ , carry the new expanding forces downward and become the matter of the new universe. The other half of the new particle,  $N/2$ , also carries the new expanding forces upward and becomes the substance of the new universe. Therefore, the emergence of astronomical black holes is a process of evolution or mutation from the old universe to the new universe. It appears that the spatial structure of a tornado (**Figure 1(b)**) resembles half of the spatial structure of an astronomical black hole (**Figure 1(a)**). The visible tornado is a funnel-shaped vortex that rotates downward from a swirling cumulonimbus cloud disk overhead. This funnel-shaped vortex does not touch the surface (or the ground) and poses no threat to people and objects on the ground. However, when the funnel-shaped vortex touches the ground, it forms a rotated downward cloud tube and the upward ejection of ground objects in **Figure 1(b)**. The matter in the vortex tube has a tremendous energy of downward motion.



When the particles in the vortex tube reach the ground, they spin the ground soil and throw other materials upwards. The yellow part of the tornado close to the ground is from the soil and ground materials that have been rolled up by the vortex tube. The upper part of the tornado is a swirling cumulonimbus cloud disk in which swirling and contracting airflows are visible. The two horizontally rotating airflows in **Figure 1(b)** carry a large number of water vapor particles moving along the red dotted-line arrows, which have centripetal forces (black line arrows). When two centripetal forces collide orthogonally at the point  $H$ , a new high mass-energy state of matter (rain and hails) is formed. At the same time, the new forces drive the new particles (rains and hails) which move vertically upward and downward.

At the Second Asian Conference of Fluid Mechanics held in Beijing on 25-29 October 1983, Wang Shizhong gave a talk in Session E2, who graduated from Southwest Associated University in China and majored in physics. His report title in this conference is “The Initial Cause Changes in Atmospheric Motion”. The theme of the report proposed a concept of updraft force. He was saying that there is a force in the atmosphere that causes the air parcels to move upward, triggering extreme precipitation and severe convective weather. However, the formation mechanism and expression of the updraft force are unknown. So, he borrowed the author of this article from the Dongtai County Meteorological Station to study the updraft force in the chief engineer’s office of the Jiangsu Provincial Meteorological Bureau for three years. This exploration has taken 40 years since 1983. Now, it has been found that the updraft force in the atmospheric motion is the new force of Equation (4) [1] [24]. In **Figure 1(b)**, the upward acceleration of wet airflows excited by the updraft force is not visible to eyes, but the about 10-km height of the rotating convective cloud like spin jets in the upper part of the rotating cumulonimbus cloud disk can be detected by radar echoes [20]. The downward acceleration with the rotating wet airflows is the tornado also like spin jets that can be referred to as the downdraft force (**Figure 1(b)**). In order to commemorate the chief engineer, Wang Shizhong, the application of this new force in meteorology is called the updraft force in this paper.

### 3. High Mass-Energy Density in Tropical Cyclones and Milky Way-Like Galaxies

In **Figure 1**, there are more than two streamlines of the continuum materials on the horizontal turntable, whether it is for the formation of a black hole or a tornado. In the open ocean, when a tropical cyclone reaches its strongest, it can form four cloud-rain bands with inward rotation and contraction (red dotted-line arrows in **Figure 2(a)**). Some of the particles on these four streamline airflows have centripetal forces. They collide orthogonally at the point  $H$  to form a more concentrated high mass-energy density. The high mass-energy density of the orthogonal interaction of the horizontal wet airflows expands from the point  $H$  and then forms a high mass-energy ring. This high mass-energy ring is the cloud-rain wall or the

outflow cloud shield of super strong tropical cyclones [28] [29], which is a ring corresponding to the distribution of the updraft force. According to Equation (4), the orthogonal interaction of the centripetal forces of the particles in the bending and contracting airflows results in upward and downward forces. The center of a strong tropical cyclone is a clear sky area formed by the downdraft force. In fact, the cloud-rain wall (or ring) in **Figure 2(a)** is the result of the centripetal force interaction of particles in different wet airflows. The cloud-rain ring visible to artificial satellites is also the result of the updraft force formed by the centripetal force interaction of airflow particles in the atmosphere. Outside the cloud-rain wall, there is a strong wind belt. In the description of wind meteorology [30], a mature tropical cyclone consists of four zones on a rotated horizontal disk: (1) an external region with wind speed increasing towards the interior and limited convection; (2) a belt, in the internal portion of which the wind reaches hurricane intensity, with gale lines and intense convection; (3) a ring that is the seat of strong precipitations, gales and maximum speed; (4) the eye, inside of which a quick drop of the speed takes place in the direction of the center.

In **Figure 2(b)**, the spatial structure of a Milky Way-like nebula system is similar as that of the tropical cyclone in **Figure 2(a)**. There are several spiral nebula bands indicated by the red-dashed arrows in **Figure 2(b)**. Those nebula particles along their curved bands have local centripetal forces indicated by the black arrows. These centripetal forces interact at the point H and form high mass-energy density. There are a large number of nebulae systems in the universe so that they rotate like the distribution in **Figure 2(b)**. In the Earth's atmosphere, there are multiple storm systems in the form of **Figure 2(a)** every day. Other

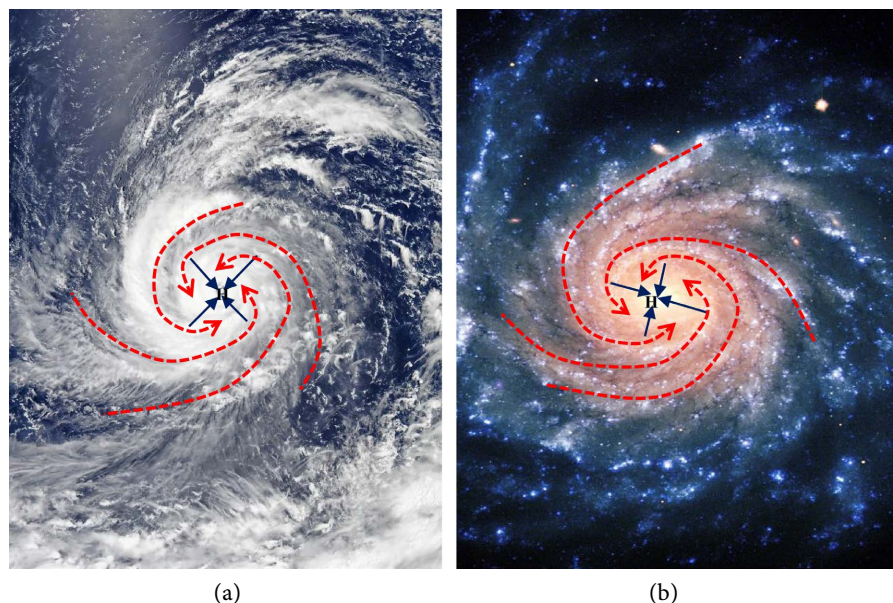


**Figure 2.** Top view of (a) a tropical cyclone and (b) a Milky Way-like nebula system. There are four spiral cloud-rain bands (red-dashed arrows) in (a) and four spiral nebula bands (red-dashed arrows) in (b). The letter H indicates the area of high energy density formed. The black arrow indicates the centripetal force.



planets and moons with atmospheres also have storm systems similar to **Figure 2(a)**. **Figure 2** shows an accretion disk of nebula materials or airflows in **Figure 1**.

We can investigate the high energy density formed by the interaction of horizontal anomalous airflows in the atmosphere. In meteorology, it has been found that extreme precipitation and severe convective weather events are the result of anomalous energy rapidly released when anomalous energy accumulates to a certain extent in the atmosphere [31]. Therefore, the anomalous component of atmospheric variables can be used to determine the type, location, intensity, and timing of extreme weather events that occurred [32]. A total variable such as wind  $v$  can be physically decomposed as climatological component  $\tilde{v}$  and anomalous component  $v'$ ,

$$v_{(d,y)}(\lambda, \varphi, p, t) = \tilde{v}_d(\lambda, \varphi, p, t) + v'_{(d,y)}(\lambda, \varphi, p, t) \quad (12)$$

where, the climatological component  $\tilde{v}_d(\lambda, \varphi, p, t) = \frac{\sum_{y=1}^M v_{(d,y)}(\lambda, \varphi, p, t)}{M}$  at a point  $(\lambda, \varphi, p, t)$  of time and space on a calendar day ( $d$ ) of year ( $y$ ) is averaged by  $M$ -year dataset of observation or reanalysis. The climatology physically varies with a daily 24-hour cycle and an annual 365-day cycle as the altitude angle of the Sun changes locally. The extreme precipitation requires two conditions: abnormal moisture (positive anomalous specific humidity or wet airflow) and vertical airflow velocity. The vertical airflow velocity is still a quantity that is difficult to determine in current numerical models [33].

From Equation (5), the updraft force modulus associated with total specific humidity ( $q_A, q_B$ ) and total wind ( $v_A, v_B$ ) is,

$$\tau_{qv} = (q_A v_A^2) \cdot (q_B v_B^2) \cdot \sin \theta. \quad (13)$$

The updraft force modulus associated with total specific humidity ( $q_A, q_B$ ) and anomalous airflows ( $v'_A, v'_B$ ) is,

$$\tau_{qv'} = (q_A v'^2_A) \cdot (q_B v'^2_B) \cdot \sin \theta. \quad (14)$$

For anomalous variable components, the updraft force modulus associated with anomalous specific humidity ( $q'_A, q'_B$ ) and anomalous airflows ( $v'_A, v'_B$ ) is,

$$\tau_{q'v'} = (q'_A v'^2_A) \cdot (q'_B v'^2_B) \cdot \sin \theta. \quad (15)$$

Three datasets are used in the calculation from Equation (13) to Equation (15). The first is the ERA-Interim reanalysis data [34] which can be downloaded from the website

(<https://www.ecmwf.int/en/forecasts/datasets/reanalysis-datasets/era-interim>)

and used to calculate hourly climatological state for the 30-year (1981-2010) period. The second is the model products of ensemble forecasts for 51 members, which can be accessed from “The International Grand Global Ensemble” project (TIGGE, <http://apps.ecmwf.int/datasets/data/tigge/levtype=pl/type=cf/>). The third is the hourly precipitation based on satellite estimate which can visit at the website

(<https://www.ncei.noaa.gov/products/climate-data-records/precipitation->

[cmorph](#)) with a horizontal resolution of 0.25 longitude-latitude grid degrees [35].

**Figure 3** shows the vertical profiles of geopotential height anomaly and temperature anomaly passing through the centers of a typhoon and a hurricane respectively. **Figure 3(a)** is the temperature anomaly after the Typhoon Megi (2010) entered the South China Sea and before it made landfall in China [9] [31]. Its lowest center (Lm) of air pressure is at the sea surface, but its center (Wm) of temperature anomaly (above 10 K) is at the tropopause (near 10 km and 300 hPa). The anomalous energy concentrated at the tropopause is partly the result of the orthogonal collision of horizontal maximum anomalous airflows with the centripetal forces in the upper troposphere. **Figure 3(b)** shows the vertical anomalous temperature profile of the Hurricane Sandy (2012) [11]. Similar result also showed that the lowest center (L0) of anomalous air pressure is located at the sea surface and the highest temperature anomaly (W2) is at the tropopause near the 300 hPa for the hurricane.

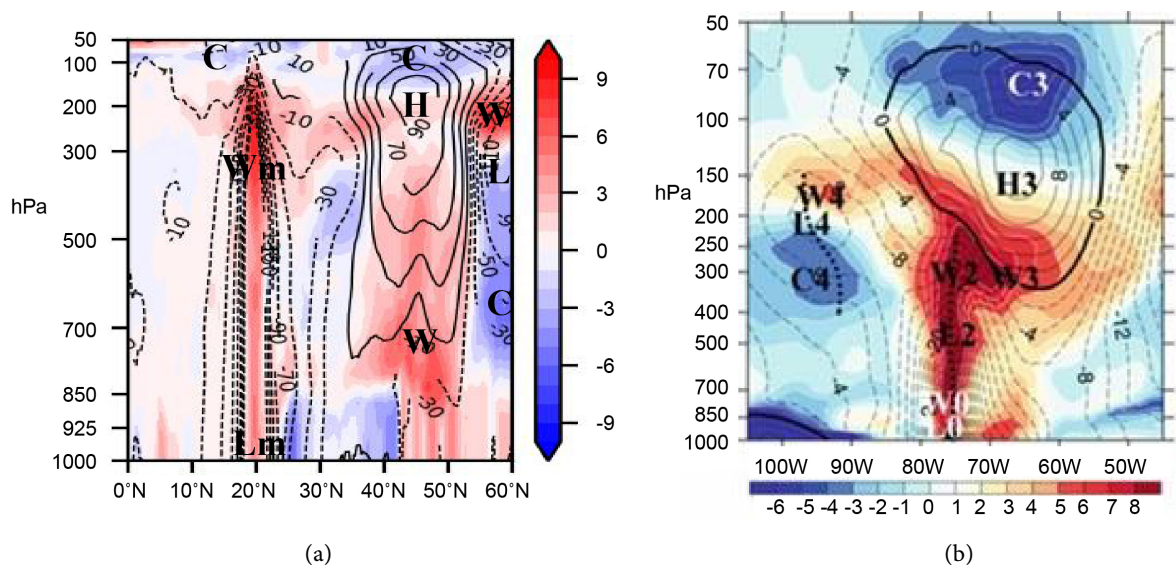


**Figure 3.** Vertical sections of geopotential height anomaly (contour,  $2 \times 10$  gpm interval) and temperature anomaly (shading, 2 K interval) based on the ERA-Interim reanalysis along tropical cyclone centers. (a) Typhoon Megi along 117.75°E at 0600 UTC on 21 October 2010. (b) Hurricane Sandy along 30°N at 1800 UTC on 27 October 2012. Letters H/L indicate the positive/negative centers of geopotential height anomaly and letters W/C are the positive/negative centers of temperature anomaly.

#### 4. Updraft Force in the Wet Atmosphere with Extreme Precipitation

Climatologically, atmospheric wind speed increases with the increase of relative ground height, and water vapor content decreases with the increase of altitude. The height of the maximum water vapor anomaly (specific humidity anomaly) is mainly concentrated around 850 hPa (1.5 km above sea level). Extreme precipitation simultaneously requires water vapor condition and vertical motion condition (upward airflow), so **Figures 4(b)-4(d)** show the spatial distributions of the

updraft force only at the 850 hPa layer. **Figure 4(a)** is the spatial distribution of hourly precipitation at 1200 UTC on 4 January 2023. It is the precipitation associated with the upward/downward airflows within the area of updraft/downdraft force and formed by an extratropical cyclone in the Northeast Pacific Ocean. At 1200 UTC (**Figure 4(a)**), a 7 mm band of hourly precipitation arrived San Francisco. It can be seen in **Figure 4**, the storm will soon make the landfall in California, creating extreme precipitation and strong winds.

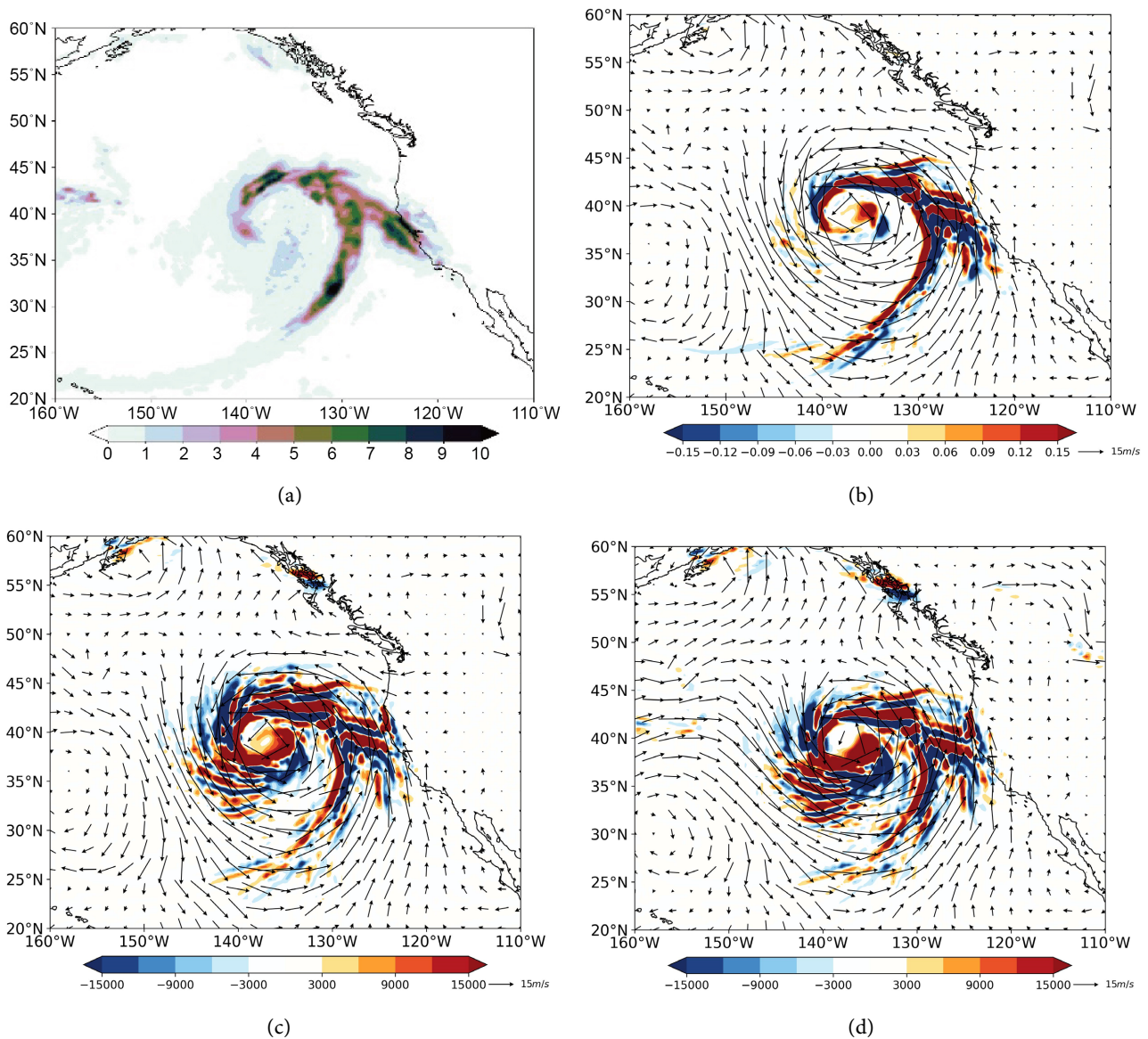


**Figure 4.** (a) Precipitation amount (mm/h) based on the CMORPH satellite estimate at 1200 UTC on 4 January 2023 [1], (b) the updraft force modulus  $\tau_{q'v'}$  (shading,  $0.03 \text{ m}^4 \cdot \text{s}^{-4} \cdot \text{kg}^{-2} \cdot \text{kg}^{-2}$  interval) associated with anomalous specific humidity  $q'$  and anomalous wind  $v'$  [1], (c) the updraft force modulus  $\tau_{qv'}$  (shading,  $1500 \text{ m}^4/\text{s}^4$  interval) associated with total specific humidity  $q$  and anomalous wind  $v'$ , and (d) the updraft force modulus  $\tau_{qv}$  (shading,  $3000 \text{ m}^4/\text{s}^4$  interval) associated with total wind  $v$  and total specific humidity  $q$  at 850 hPa at 1200 UTC on 4 January 2023. Anomalous winds (m/s) are shown in (b) and (c) but total wind (m/s) in (d).

**Figure 4(b)** is the updraft force modulus  $\tau_{q'v'}$ , which is associated with the anomalous specific humidity (wet airflow)  $q'$  and anomalous wind  $v'$ . It can be noted that the updraft force modulus  $\tau_{q'v'}$  is well correlated with the precipitation from intensity and coverage. In **Figure 4(b)**, the red and blue shadings indicate the updraft force and the downdraft force of wet airflows at the moment of 1200 UTC on 4 January 2023. Usually, updraft force and downdraft force are close together in pairs. In the hail convective cloud model, strong updraft and downdraft motions occur in pairs [36] [37]. Heavy precipitation occurs in an updraft area and hail occurs in adjacent downdraft area. Comparing **Figure 4(a)** and **Figure 4(b)**, it can be seen that the updraft/downdraft force associated with anomalous specific humidity  $q'$  and anomalous wind  $v'$  can be used to indicate extreme precipitation from its intensity and coverage. If considering total specific humidity, the coverage and intensity of updraft force modulus ( $\tau_{qv'}$ ) associated with anomalous wind in **Figure 4(c)** are larger and stronger than that shown in Figure 4b indicated by the updraft force modulus  $\tau_{q'v'}$ , while the later considers anomalous specific humidity and anomalous wind conditions. The coverage and intensity of updraft force modulus ( $\tau_{qv}$ ) associated with total wind and total specific humidity (**Figure 4(d)**) are also larger and stronger than that ( $\tau_{qv'}$ ) associated with only anomalous wind (**Figure 4(c)**).

In **Figure 4(b)**, the red and blue shadings are like squall lines caused by the updraft force and the downdraft force. The squall line is a line of thunderstorm cells or strong winds due to instability associated with the updraft force and the downdraft force. They are short-lived, are accompanied by thunder, lightning and precipitations, and occur along the front of a cyclone [30].

## 5. Discussion

In nature, matter or particles move in a curvilinear motion in the universe so that they have centripetal forces. It is the curvilinear motion of these particles that cause the interaction or collision between particles to occur. Two particles interacting or colliding under centripetal forces can have different angles. Among them, the 90-degree interaction of the two centripetal forces of the motion of two particles is called an orthogonal collision. The orthogonal collision forms the highest mass-energy density at the collision point. The orthogonal collision of old matter or old particles with the centripetal forces can form new states of matter and new particles. Old and new particles belong to two different universes or two different worlds. In the new universe or new world, there is only information about new particles which can satisfy the conservation of mass and the conservation of energy. We cannot find any information of the old universe in the new universe. The total mass-energy respectively in the old universe and the new universe is equal. However, the total mass or total energy in the old universe is not equal to that in the new universe. The centripetal forces of two airflows or two particles moved interactively in the old universe form a plane. As a result of the orthogonal collision of two old particles with their centripetal forces, not only the

new state of matter and high energy density are formed, but also a large number of new particles are equally distributed on both sides of the collision plane. These new particles are expanding at an accelerated pace in the new universe. Each new particle is acceleration under the action of the expanding force after the collision so that has two moving components: the straight-line acceleration and bending movement. All the new particles make up the overall expansion of space in the new universe and the contraction or convergence of new particles in local areas, forming new celestial bodies, such as black holes, stars, planets, moons, and even rotating celestial bodies like the Milky Way. The universe expansion and these phenomena or observational facts are some interactive results of new particles with straight-line acceleration and bending motion after the Big Bang.

At the orthogonal collision point of the old particles, not only a high mass-energy density similar to an astronomical black hole is formed, but also new matter or new particles are formed that are thrown at both sides of the collision plane with acceleration. High energy spin jets are formed outwards at the two poles of the black hole on both sides of the collision plane. The formation of an astronomical black hole is not just an orthogonal collision of two old particles with their centripetal forces, but the orthogonal collisions of multiple rotating particle bands with their centripetal forces. Multiple rotating old particle bands form an accretion disk. The new particles in the upward and downward high energy spin jets have expanding forces instead of the gravitational force statistically given by the Newton's law. Spin jets and black holes are two parts of a phenomenon (extreme event) formed simultaneously by the orthogonal collision of bending and rotating particles associated with their centripetal forces. It means that spin jets are not created by supermassive black holes through the particle gravity. The free fall of an apple from a tree is a natural phenomenon. The Newton's story said that this natural phenomenon is the seduction of gravity from the Earth's center. However, the orthogonal collision theory says that it is the particle acceleration caused by the expanding force since the Big Bang after the earliest orthogonal collision. The expansion of the universe is an observational fact. Gravitational force is people's subjective description or intuition of an objective phenomenon. The physical essence of gravity is the force of expansion after the Big Bang.

The above phenomenon summarizes the natural extremes on the astronomical scale. On the meteorological scale, a tornado formed under a rotating cumulonimbus cloud disk which is like an accretion disk around an astronomical black hole. The orthogonal collision of the particles under the centripetal forces in the rotating airflows in the cumulonimbus cloud disk forms a high mass energy density in the new state of matter. The upward acceleration of the new particles is the result of the updraft force, vertically showing a deep (more than 10 km) convection cloud which can be detected by meteorological radars. The downward acceleration of the new particles is the result of the downdraft force, which can form a tornado to touch the ground and produce disaster.

The updraft and downdraft forces in the atmosphere are the dynamic



conditions for the formation of extreme precipitation and severe convective weather events. Since the development of meteorology, the accurate measurement and calculation of vertical motion in the atmosphere have been an unsolved problem. The second condition for extreme precipitation is anomalous specific humidity which is mainly concentrated in the lower troposphere. Therefore, the physical quantities calculated from the anomalous specific humidity and the updraft force of anomalous winds (or anomalous airflows) on the 850 hPa horizontal layer can indicate the time, location and intensity of extreme precipitation appeared. The expanding force in the orthogonal collision theory can be applied not only to the description of extreme phenomena at the astronomical scale and meteorological scale, but also to the description of extreme phenomena at the microscopic scale. These microscopic extremes include the aurora phenomenon in the Earth's upper atmosphere and the new state of matter formed by the orthogonal collision collider [25] [38].

**Figure 1** shows the two spatial-scale structures of extreme events or phenomena respectively from astronomical scale and meteorological scale. The spatial structure of their spin jets is similar as a funnel-shaped vortex. Recently combination of black hole property for elementary particles, such as electron, and quantum mechanics at the Planck scale (the microscopic scale) also showed the spin jets [39] similar to the funnel-shaped vortex in **Figure 1(a)**. This structure can be also imagined for elementary particles with jet energies constructing their spin and Planck mass-energy distribution. In the schematic presentation of Planck scale-based electron black hole [39], the initial electron soup is made up of elementary particles, similar as the nebula materials in **Figure 1(a)** on the accretion disk and the cumulonimbus cloud disk in **Figure 1(b)**. Two spin jets exist in two polar directions outside an electron black hole. The question is worth looking into whether is the same process of the formation for the three-type black holes with their jets at different scales. On the astronomical scale, a black hole has too long a time and too large a space. On the Planck scale, an electron black hole has too short a time and too small a space. The quantitative study of black holes at the above two scales is extremely difficult. On the meteorological scale, however, black holes like tornadoes and tropical cyclones can be quantitatively studied in time and space by human on Earth.

The updraft force in the orthogonal collision theory can not only be applied to predict extreme precipitation and severe convective weather events in the field of meteorology [24], but also to explain the uplift of mountain ranges in the field of geology, such as the uplift of the Tibet Plateau [40]. The uplift force formed by the centripetal forces of the horizontal movement of upper magmatic fluids during the early Earth period [41] is different from the “crustal stress” proposed by Li Siguang [42]. The uplift force in magmatic fluids during the early Earth period was similar to the updraft force in the atmosphere. Extreme precipitation and severe convective weather events in the atmosphere mainly occur on anomalous wind shear lines in the low-level wet atmosphere [31]. Of course, the updraft force



cannot be simply understood as the shear stress of anomalous winds along the convergence lines of horizontal anomalous airflows [1] [24].

Can the orthogonal collision theory fully explain all kinds of extreme phenomena in nature for all time-space scales? The Big Bang may be the highest mass-energy density distribution formed by the orthogonal collision of the curvilinear motion of large particles associated with the centripetal forces in the old universe for the cosmological scale. The process shows that the expanding force since the Big Bang forms an expansion of the thermodynamic energy gradient into outer space. Therefore, the new particles in the new universe have straight-line accelerations and curvilinear centripetal forces, which show the dynamic characteristics of the expansion of the new universe. These new particles are generally expanding in space, but due to curvilinear motion, local particles converge and collide, forming new celestial bodies, such as stars, planets, satellites and other interstellar material phenomena. The particles that make up each star or each celestial body still have the expanding force since the Big Bang so that their target is going to the center point of each star (or each planet or each moon), which appears to be the Newtonian gravity. Thus, two different worldviews try to explain the same natural phenomenon.

If the atmosphere on the Earth's surface is heated by the underlying surface, the difference in heating will inevitably form an abnormal horizontal temperature gradient, so the result is that the centripetal force of the bending movement of the abnormal airflows (winds) forms extreme weather phenomena such as tornadoes and extreme precipitation. The Big Bang, tornadoes, and new celestial bodies are all newly formed extreme events or phenomena. There is a logical relationship namely "Heating differences first produce wind anomalies and then the wind anomalies generate extreme events such as rainfall and tornadoes". This logical relationship of nature can also be applied in the formation of micro-scale extreme events, such as unlike charges (separation of positive and negative charges) generated by the relative motion between adjacent cloud bodies with different temperatures. Nuclear fusion (collision of energetic particles) on stars also satisfies the logical relationship. For example, thermodynamic differences on the Sun create new extreme events of sunspots through the interaction or collision of energetic particles. When people scientifically understand this logical relationship, they can not only avoid natural disasters from the above three scales, but also benefit mankind. The orthogonal collision theory attempts to explain all kinds of extreme phenomena in nature by using all kinds of energy and forces.

## 6. Conclusions

This paper explores a novel theory, orthogonal collision theory, to explain extreme phenomena in both astronomy (e.g., black holes, nebula systems) and meteorology (e.g., tornadoes, tropical cyclones). The central claim is that these phenomena, despite their differences in time-space scales, share similar underlying dynamical mechanisms based on the interaction or collision of old particles associated with

centripetal forces in rotating, contracting systems so that they form accretion disks. The earliest extreme event is the Big Bang. This universal and original phenomenon at the cosmological scale was caused by the two large bodies or two old particles through orthogonal interaction (or collision) of their centripetal forces. Thus, this comprehensive framework seeks to unify the understanding of diverse extreme events in multiple time-space scales.

Two new forces of expanding force and updraft force are presented in this paper. The physical essence of two forces is really the same. The expanding force is used in astronomy, the updraft force is used in meteorology and the uplift force is used in geology. They may have other new forces existed in different scientific fields. All new forces are caused by old particles interacted or collided orthogonally through the centripetal forces of old particles with bending motions. In the field of high-energy physics or quantum physics, the old particle interaction associated with centripetal forces leads to new high-energy states (or produce new particles) with new spin jets. The new spin jets show the form of expanding force at the Planck scale. The interaction of centripetal forces in other scientific fields has led to the formation of new states of matter, such as extreme precipitation in meteorology and mountain uplift in geology. In fact, the orthogonal collision theory attempts to give a single dynamical mechanism, offering insights into natural processes and phenomena across disciplines.

## Acknowledgements

The author wishes to thank the three anonymous reviewers for constructive suggestions and comments and criticisms which have improved the paper and confirmed the orthogonal collision theory. This work was supported by the National Natural Science Foundation of China (Grant Number: 41775067).

## Conflicts of Interest

The author declares no conflicts of interest regarding the publication of this paper.

## References

- [1] Qian, W. (2024) The Essence of Gravity Is the Expansion Tendency of the Universe after the Big Bang. *Journal of Modern Physics*, **15**, 804-849. <https://doi.org/10.4236/jmp.2024.156036>
- [2] Shi, L., Olabarrieta, M., Nolan, D.S. and Warner, J.C. (2020) Tropical Cyclone Rainbands Can Trigger Meteotsunamis. *Nature Communications*, **11**, Article No. 678. <https://doi.org/10.1038/s41467-020-14423-9>
- [3] Camargo, S.J. and Wing, A.A. (2021) Increased Tropical Cyclone Risk to Coasts. *Science*, **371**, 458-459. <https://doi.org/10.1126/science.abg3651>
- [4] Sejnowski, T.J. (1969) Effect of a Black Hole on Stellar Dynamics. *Bulletin of the American Physical Society*, **14**, 616.
- [5] Ruffini, R. and Wheeler, J.A. (1971) Introducing the Black Hole. *Physics Today*, **24**, 30-41. <https://doi.org/10.1063/1.3022513>
- [6] Agee, E., Church, C., Morris, C. and Snow, J. (1975) Some Synoptic Aspects and

- Dynamic Features of Vortices Associated with the Tornado Outbreak of 3 April 1974. *Monthly Weather Review*, **103**, 318-333.  
[https://doi.org/10.1175/1520-0493\(1975\)103<0318:ssaadf>2.0.co;2](https://doi.org/10.1175/1520-0493(1975)103<0318:ssaadf>2.0.co;2)
- [7] Corfidi, S.F., Weiss, S.J., Kain, J.S., Corfidi, S.J., Rabin, R.M. and Levit, J.J. (2010) Revisiting the 3-4 April 1974 Super Outbreak of Tornadoes. *Weather and Forecasting*, **25**, 465-510. <https://doi.org/10.1175/2009waf2222297.1>
  - [8] Knupp, K.R., Murphy, T.A., Coleman, T.A., Wade, R.A., Mullins, S.A., Schultz, C.J., et al. (2014) Meteorological Overview of the Devastating 27 April 2011 Tornado Outbreak. *Bulletin of the American Meteorological Society*, **95**, 1041-1062.  
<https://doi.org/10.1175/bams-d-11-00229.1>
  - [9] Qian, W., Shan, X., Liang, H., Huang, J. and Leung, C. (2014) A Generalized Beta-advection Model to Improve Unusual Typhoon Track Prediction by Decomposing Total Flow into Climatic and Anomalous Flows. *Journal of Geophysical Research: Atmospheres*, **119**, 1097-1117. <https://doi.org/10.1002/2013jd020902>
  - [10] Chen, N., Han, G., Yang, J. and Chen, D. (2014) Hurricane Sandy Storm Surges Observed by HY-2A Satellite Altimetry and Tide Gauges. *Journal of Geophysical Research: Oceans*, **119**, 4542-4548. <https://doi.org/10.1002/2013jc009782>
  - [11] Qian, W., Huang, J. and Du, J. (2016) Examination of Hurricane Sandy's (2012) Structure and Intensity Evolution from Full-Field and Anomaly-Field Analyses. *Tellus A: Dynamic Meteorology and Oceanography*, **68**, Article No. 29029.  
<https://doi.org/10.3402/tellusa.v68.29029>
  - [12] Lehoux, D. (2020) Cosmology and Meteorology. In: Mitsis, P., Ed., *Oxford Handbook of Epicurus and Epicureanism*, Oxford University Press, 81-93.  
<https://doi.org/10.1093/oxfordhb/9780199744213.013.7>
  - [13] Akiyama, K., Alberdi, A., Alef, W., et al. (2019) First M87 Event Horizon Telescope Results. I. The Shadow of the Supermassive Black Hole. *The Astrophysical Journal Letters*, **875**, L1.
  - [14] Akiyama, K., Alberdi, A., Alef, W., et al. (2022) First Sagittarius A\* Event Horizon Telescope Results. I. The Shadow of the Supermassive Black Hole in the Center of the Milky Way. *The Astrophysical Journal Letters*, **875**, L12.
  - [15] Simmons, K.M. and Sutter, D. (2012) The 2011 Tornadoes and the Future of Tornado Research. *Bulletin of the American Meteorological Society*, **93**, 959-961.  
<https://doi.org/10.1175/bams-d-11-00126.1>
  - [16] Penrose, R. (1965) Gravitational Collapse and Space-Time Singularities. *Physical Review Letters*, **14**, 57-59. <https://doi.org/10.1103/physrevlett.14.57>
  - [17] Schwarzschild, K. (2003) "Golden Oldie": On the Gravitational Field of a Mass Point According to Einstein's Theory. *General Relativity and Gravitation*, **35**, 951-959.  
<https://doi.org/10.1023/a:1022971926521>
  - [18] Schaefer, J.T. and Edwards, R. (1999) The SPC Tornado/Severe Thunderstorm Database. 11<sup>th</sup> Conference on Applied Climatology, Dallas, 10-15 January 1999, 603.
  - [19] Schultz, D.M., Richardson, Y.P., Markowski, P.M. and Doswell, C.A. (2014) Tornadoes in the Central United States and the "Clash of Air Masses". *Bulletin of the American Meteorological Society*, **95**, 1704-1712.  
<https://doi.org/10.1175/bams-d-13-00252.1>
  - [20] Qian, W.H., Leung, J., Jin, R.H., et al. (2017) Application of Anomalous Variables in Severe Convection System Analyses and Model Evaluation: A Case Study on Tornado-Producing Anomalous Systems near Lixiahe Basin, Jiangsu Province. *Meteorological Monthly*, **43**, 129-143.

- [21] Chakrabarti, S.K. (2001) Jets and Outflows from Advective Accretion Disks. *AIP Conference Proceedings*, **558**, 246-257. <https://doi.org/10.1063/1.1370795>
- [22] Rasmussen, E.N. and Straka, J.M. (2007) Evolution of Low-Level Angular Momentum in the 2 June 1995 Dimmitt, Texas, Tornado Cyclone. *Journal of the Atmospheric Sciences*, **64**, 1365-1378. <https://doi.org/10.1175/jas3829.1>
- [23] Qian, W. (2023) Identifying the Spatial Structure of Black Hole and Tropical Cyclone Based on a Theoretical Analysis of Orthogonal Interaction. *Journal of Modern Physics*, **14**, 933-952. <https://doi.org/10.4236/jmp.2023.146052>
- [24] Qian, W., Du, J., Leung, J.C., Li, W., Wu, F. and Zhang, B. (2023) Why Are Severe Weather and Anomalous Climate Events Often Associated with the Orthogonal Convergence of Airflows? *Weather and Climate Extremes*, **42**, Article ID: 100633. <https://doi.org/10.1016/j.wace.2023.100633>
- [25] Qian, W. (2022) Orthogonal Collision of Particles Produces New Physical State. *Journal of Modern Physics*, **13**, 1440-1451. <https://doi.org/10.4236/jmp.2022.1311089>
- [26] Einstein, A. (1905) Does the Inertia of a Body Depend upon Its Energy-Content? *Annalen der Physik*, **323**, 639-641. <https://doi.org/10.1002/andp.19053231314>
- [27] Qian, W. (2023) A Physical Interpretation of Mass-Energy Equivalence Based on the Orthogonal Collision. *Journal of Modern Physics*, **14**, 1067-1086. <https://doi.org/10.4236/jmp.2023.147059>
- [28] Mathur, M.B. (1998) Development of an Eye-Wall like Structure in a Tropical Cyclone Model Simulation. *Dynamics of Atmospheres and Oceans*, **27**, 527-547. [https://doi.org/10.1016/s0377-0265\(97\)00029-8](https://doi.org/10.1016/s0377-0265(97)00029-8)
- [29] Corbosiero, K.L., Molinari, J., Ayyer, A.R. and Black, M.L. (2006) The Structure and Evolution of Hurricane Elena (1985). Part II: Convective Asymmetries and Evidence for Vortex Rossby Waves. *Monthly Weather Review*, **134**, 3073-3091. <https://doi.org/10.1175/mwr3250.1>
- [30] Solari, G. (2019) Wind Meteorology, Micrometeorology and Climatology. In: Solari, G., Ed., *Wind Science and Engineering: Origins, Developments, Fundamentals and Advancements*, Springer International Publishing, 325-440. [https://doi.org/10.1007/978-3-030-18815-3\\_6](https://doi.org/10.1007/978-3-030-18815-3_6)
- [31] Qian, W.H. (2017) Temporal Climatology and Anomalous Weather Analysis. Springer Atmospheric Sciences. Springer, 687 p.
- [32] Qian, W., Du, J. and Ai, Y. (2021) A Review: Anomaly-Based versus Full-Field-Based Weather Analysis and Forecasting. *Bulletin of the American Meteorological Society*, **102**, E849-E870. <https://doi.org/10.1175/bams-d-19-0297.1>
- [33] Gvoždíková, B. and Müller, M. (2021) Predictability of Moisture Flux Anomalies Indicating Central European Extreme Precipitation Events. *Quarterly Journal of the Royal Meteorological Society*, **147**, 3335-3348. <https://doi.org/10.1002/qj.4131>
- [34] Dee, D.P., Uppala, S.M., Simmons, A.J., Berrisford, P., Poli, P., Kobayashi, S., et al. (2011) The ERA-Interim Reanalysis: Configuration and Performance of the Data Assimilation System. *Quarterly Journal of the Royal Meteorological Society*, **137**, 553-597.
- [35] Joyce, R.J., Janowiak, J.E., Arkin, P.A. and Xie, P. (2004) CMORPH: A Method That Produces Global Precipitation Estimates from Passive Microwave and Infrared Data at High Spatial and Temporal Resolution. *Journal of Hydrometeorology*, **5**, 487-503. [https://doi.org/10.1175/1525-7541\(2004\)005<0487:camtpg>2.0.co;2](https://doi.org/10.1175/1525-7541(2004)005<0487:camtpg>2.0.co;2)
- [36] Browning, K.A. and Foote, G.B. (1976) Airflow and Hail Growth in Supercell Storms and Some Implications for Hail Suppression. *Quarterly Journal of the Royal Meteorological*

- Society*, **102**, 499-533. <https://doi.org/10.1002/qj.49710243303>
- [37] Wang, X.M., Zhong, Q. and Han, S.Y. (2009) A Numerical Case Study on the Evolution of Hail Cloud and the Three-Dimensional Structure of Supercell. *Plateau Meteorology*, **28**, 352-365.
  - [38] Qian, W. (2023) A Physical Explanation for the Formation of Auroras. *Journal of Modern Physics*, **14**, 271-286. <https://doi.org/10.4236/jmp.2023.143018>
  - [39] Akhavan, O. (2022) The Universe Creation by Electron Quantum Black Holes. *Acta Scientific Applied Physics*, **2**, 34-45.
  - [40] Qian, W., Leung, J.C. and Zhang, B. (2023) An Orthogonal Collision Dynamic Mechanism of Wave-Like Uplift Plateaus in Southern Asia. *Open Journal of Geology*, **13**, 828-846. <https://doi.org/10.4236/ojg.2023.138037>
  - [41] Qian, W. and Du, J. (2023) A Study on the Plate Tectonics in the Early Earth Period Based on the Core-Magma Angular Momentum Exchange. *Open Journal of Geology*, **13**, 598-621. <https://doi.org/10.4236/ojg.2023.136026>
  - [42] Li, S.G. (1973) Introduction to Geomechanics. Science Press.